Supplement of Geosci. Model Dev., 12, 2401–2418, 2019
https://doi.org/10.5194/gmd-12-2401-2019-supplement
© Author(s) 2019. This work is distributed under
the Creative Commons Attribution 4.0 License.

Geoscientific Model Development
Open Access
EGU

Supplement of

Challenges in developing a global gradient-based groundwater model (G^3M v1.0) for the integration into a global hydrological model

Robert Reinecke et al.

Correspondence to: Robert Reinecke (reinecke@em.uni-frankfurt.de)

The copyright of individual parts of the supplement might differ from the CC BY 4.0 License.

Supplement

1 Coupling to WGHM

With a spatial resolution of 0.5° by 0.5° (approximately 55 km by 55 km at the equator), the WaterGAP 2 model (Alcamo et al., 2003) computes human water use in five sectors and the resulting net abstractions from GW and SW for all land areas of the globe excluding Antarctica. These net abstractions are then taken from the respective water storages in the WaterGAP Global Hydrology Model (WGHM) (Müller Schmied et al., 2014; Döll et al., 2003; 2012; 2014). With daily time steps, WGHM simulates flows among the water storage compartments canopy, snow, soil, GW, lakes, man-made reservoirs, wetlands and rivers. As in other GHMs, the dynamic of GW storage (GWS) is represented in WGHM by a linear GW reservoir model, i.e.

$$\frac{dGWS}{dt} = R_g + R_{g\_swb} - NA_g - k_g\, GWS \qquad \text{(S1)}$$

where R_g $[L^3T^{-1}]$ is diffuse GW recharge from soil, R_{g_swb} $[L^3T^{-1}]$ GW recharge from lakes, reservoirs and wetlands (only in arid and semiarid regions, with a global constant value per SW body area), NA_g $[L^3T^{-1}]$ net GW abstraction. The product $k_g\, GWS$ quantifies GW discharge to SW bodies as a function of GWS and the GW discharge coefficient k_g (Döll et al., 2014). G³M is to replace this linear reservoir model in WGHM. Capillary rise is not included in the presented steady-state simulation, as simulation of capillary rise requires information of soil moisture that is only available when G³M is fully integrated into WGHM.

G³M will be integrated into WGHM by exchanging information on (1) R_{g_swb} and NA_g, (2) soil water content, (3) Q_{cr}, (4) h_{swb}, and (5) Q_{swb}. Figure S1.1 indicates the direction of the information flows. Water flows from the 0.5° cells of WGHM are distributed equally to all 5' G³M grid cells inside a 0.5° cell. Flows transferred from the 5' cells of G³M to WGHM are aggregated. GW recharge and net abstraction from GW together with SW tables are the main drivers of the GW model that will be provided dynamically by WGHM. GW-SW flow volumes computed by G³M will be aggregated and added or subtracted from the SW body volumes in WGHM, and SW body heads will be recalculated. WGHM soil water content together with G³M WTD will be used to calculate capillary rise and thus a change of soil water content. WaterGAP includes a one layer soil water storage compartment characterized by land cover specific rooting depth, maximum storage capacity and soil texture (Döll et al., 2014). The water content in the soil storage is increased by incoming precipitation and decreased by evapotranspiration and runoff generation (Döll et al., 2014). Capillary rise is not yet implemented in G³M, and SW heads are currently based on land surface elevation.

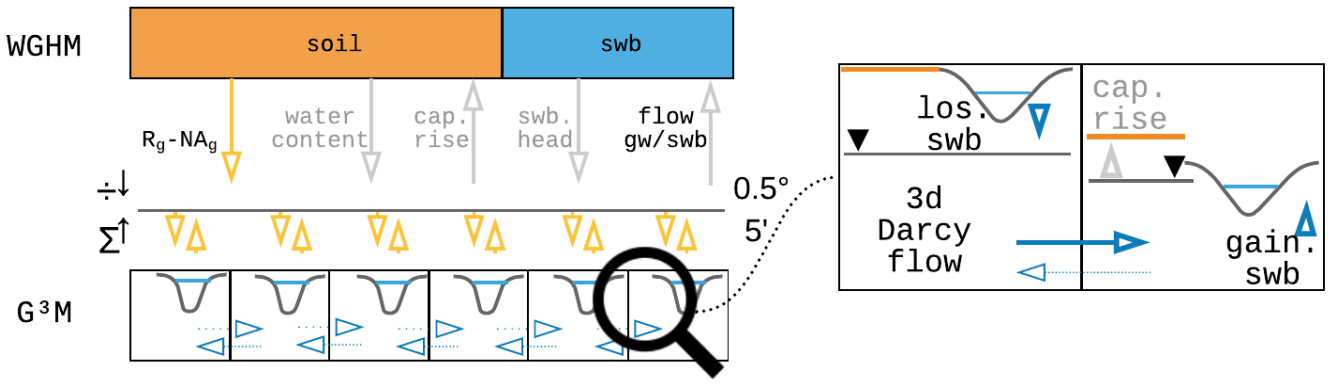

Figure S1.1 Conceptual view of the coupling between WGHM and G³M. WGHM provides calculated GW recharge (R_g) (Döll and Fiedler, 2008) and if the human impact is considered, net abstraction from GW (NA_g) (Döll et al., 2012). G³M spreads this input equally to all 5' grid cells inside a 0.5° cell and calculates hydraulic head and interactions with SW bodies (swb) as well as capillary rise (cap. rise) at the 5' resolution. Grey arrows show information flow that is not yet implemented.

2 Case study Central Valley

To evaluate G³M further, its results were analysed for to a well-studied region, the Central Valley in California, USA. The Central Valley is one of the most productive agricultural regions of the world and heavily relies on GW pumpage to meet irrigation demands (Faunt et al., 2016). GW pumping in the valley increased rapidly in the 1960s (Faunt, 2009). Figure S2.1 shows simulated WTD for the Central Valley, the coast and the neighboring Sierra Nevada mountainside as well as parts of the Great Basin. The WTD table represents natural conditions without any pumping and is rather small. It roughly resembles the WTD assumed in the Central Valley Hydrological Model (CVHM) as initial condition, representing a natural state (Faunt, 2009) (Fig. S2.1b). G³M correctly computes the shallow conditions with groundwater above the surface in the north, partially in the south of the valley and decreasing towards the Sierra Nevada. The difference in the extend of flooded area could be due to large wetlands areas still present in the early 60s which are not represented in this extent in the data used by G³M. Beyond the CVHM domain, WTD in mountainous regions is probably overestimated by G³M. The elevation of neighboring cells may differ up to a 1000 meter resulting in a large gradient (Fig. S4.5b and S4.5e).

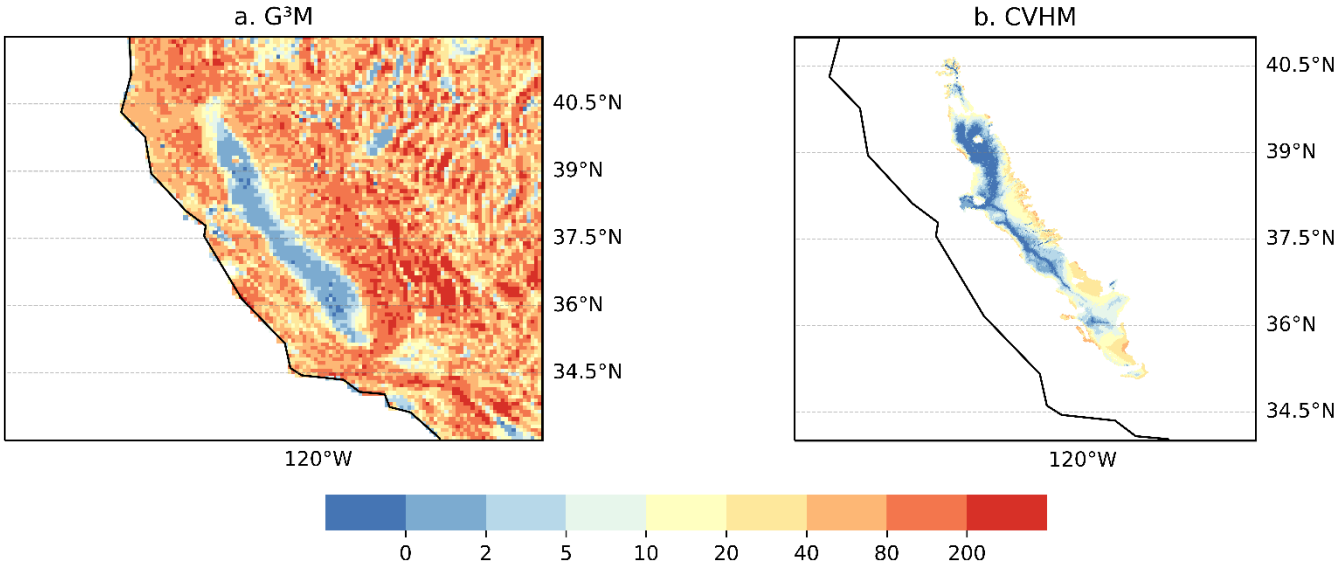

Figure S2.1 Plots of WTD [*m*] as calculated by G³M for the Central Valley and the Great Basin (a), and as used by CVHM as the natural state and starting condition (Faunt, 2009) (b).

3 Sensitivity Analysis

Sensitivities are calculated using forward differences (Poeter et al., 2014).

$$\frac{\Delta y_i'}{\Delta b_j} = \frac{y_i'(b_j + \Delta b_j - y_i'(b_j)}{\Delta bj_j} \quad \text{(S2)}$$

where y_i' is the simulated hydraulic head at position i from ND number of cells and b_j the perturbed parameter, here a multiplier for grid specific values shown in Table S1, in a vector of all parameter b of length j. Based on these values the composite scaled sensitivity is computed as

$$CSS_j = \sqrt{\sum_{i=1}^{ND} \frac{\Delta y_i'}{\Delta b_j} ND^{-1}} \quad \text{(S3)}$$

The result of the CSS is in units of meters. The higher the CSS, the more sensitive are the computed hydraulic heads to the parameter (Table S1).

Table S1 Ranges of parameter multipliers used in the local sensitivity analysis and their resulting composite scaled sensitivity values. The multiplier for the wetlands applies to global and local wetlands.

Parameter	$\boldsymbol{\Delta b}$	**Composite Scaled Sensitivity [m]**
h_{swb}	0.01	39132.1
K_{aq}	0.01	76.8
R_g	0.1	39.8
c_{Lakes}	0.1	3.2
$c_{Wetlands}$	0.1	0.014
c_{riv}	0.1	0.013
c_{ocean}	0.1	0.013

4 Additional Figures

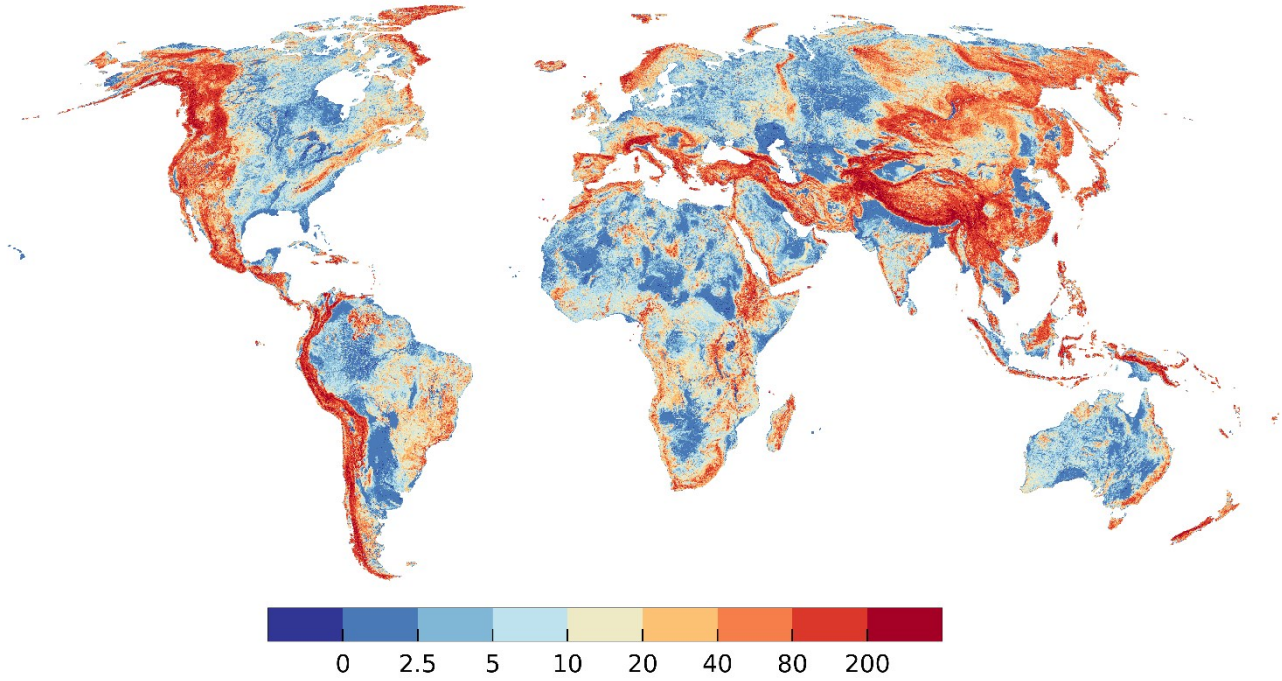

Figure S4.1 Difference [***m***] between 5' average of 30" land surface elevation and P_{30} elevation. Maximum value 1365 m**.**

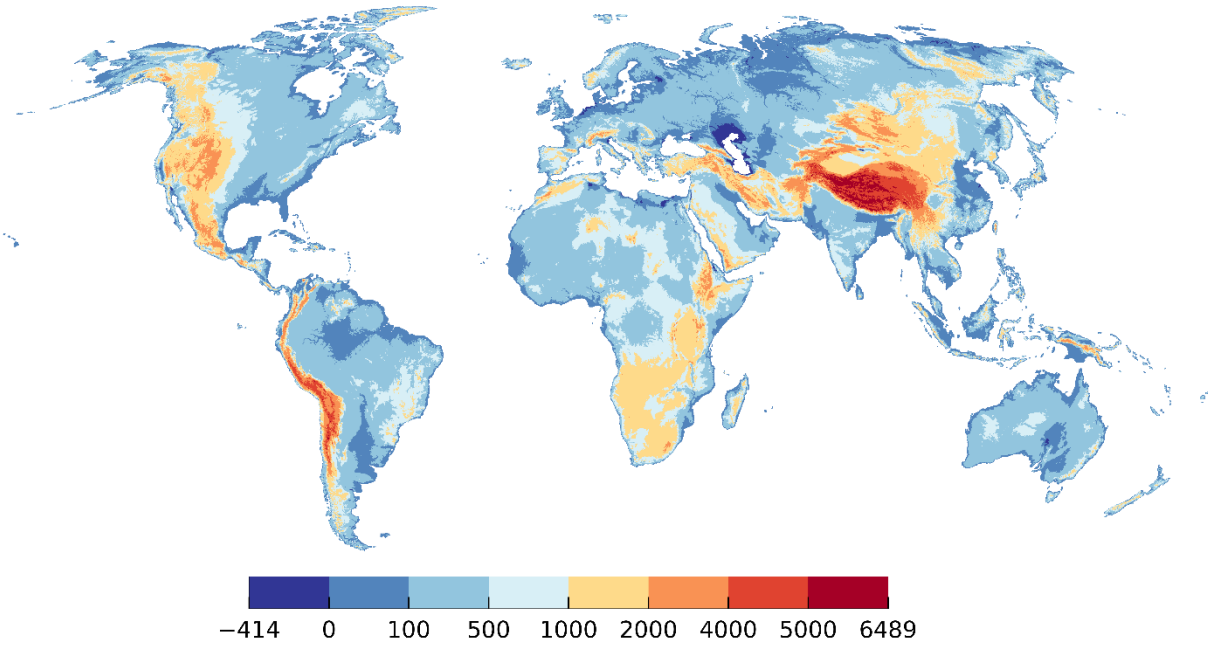

Figure S4.2 Land surface elevation [***m***] used in G³M: 5' average of 30" land surface elevation used in Fan et al. (2013).

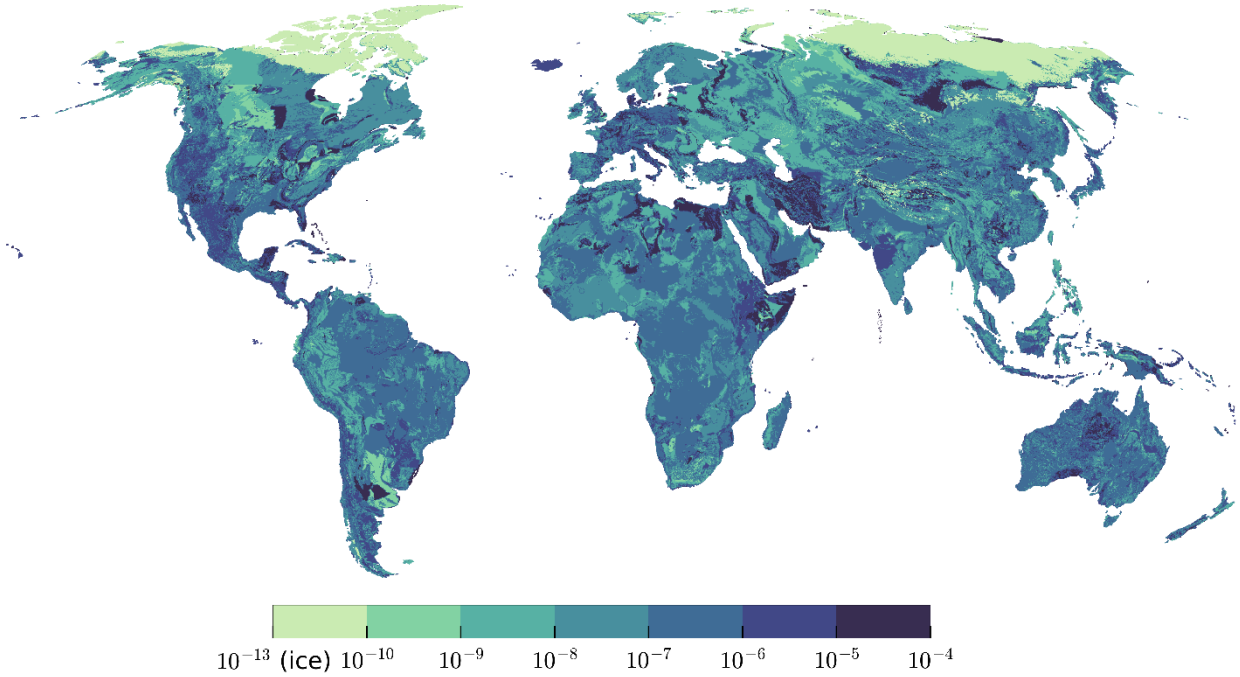

Figure S4.3 Hydraulic conductivity [$\boldsymbol{ms^{-1}}$] derived from Gleeson et al. (2014) by scaling it with the geometric mean to 5'. Very low values in the northern hemisphere are due to permafrost conditions.

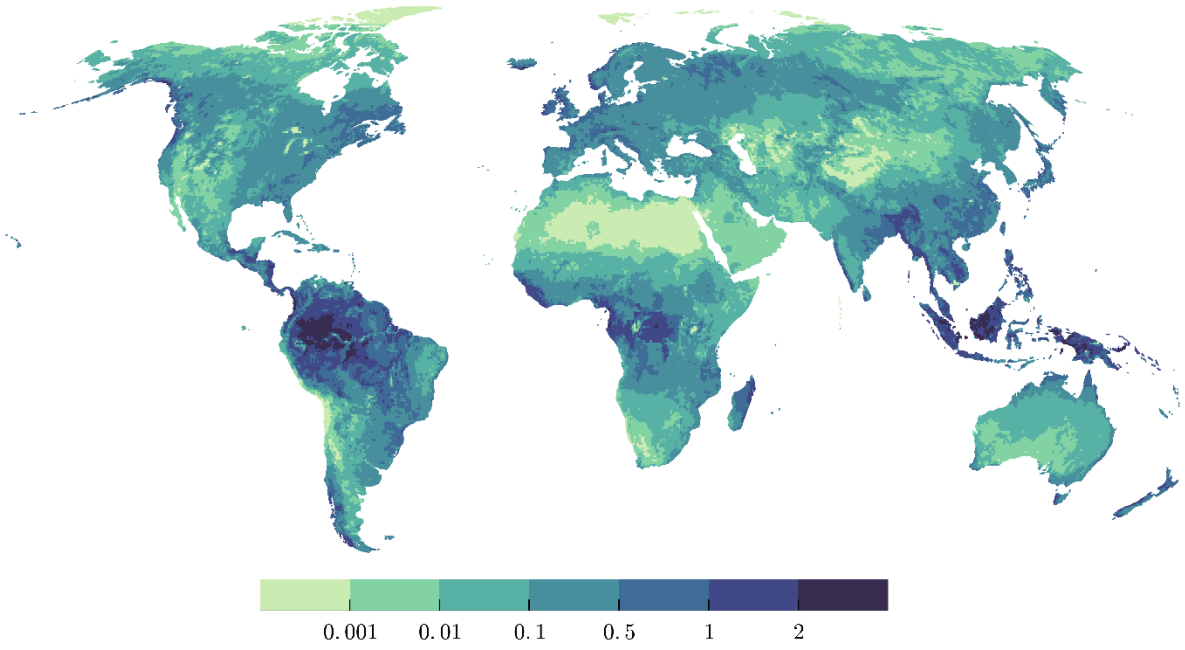

Figure S4.4 Mean annual groundwater recharge [$\boldsymbol{mm\ day^{-1}}$] between 1901-2013, from WaterGAP 2.2c.

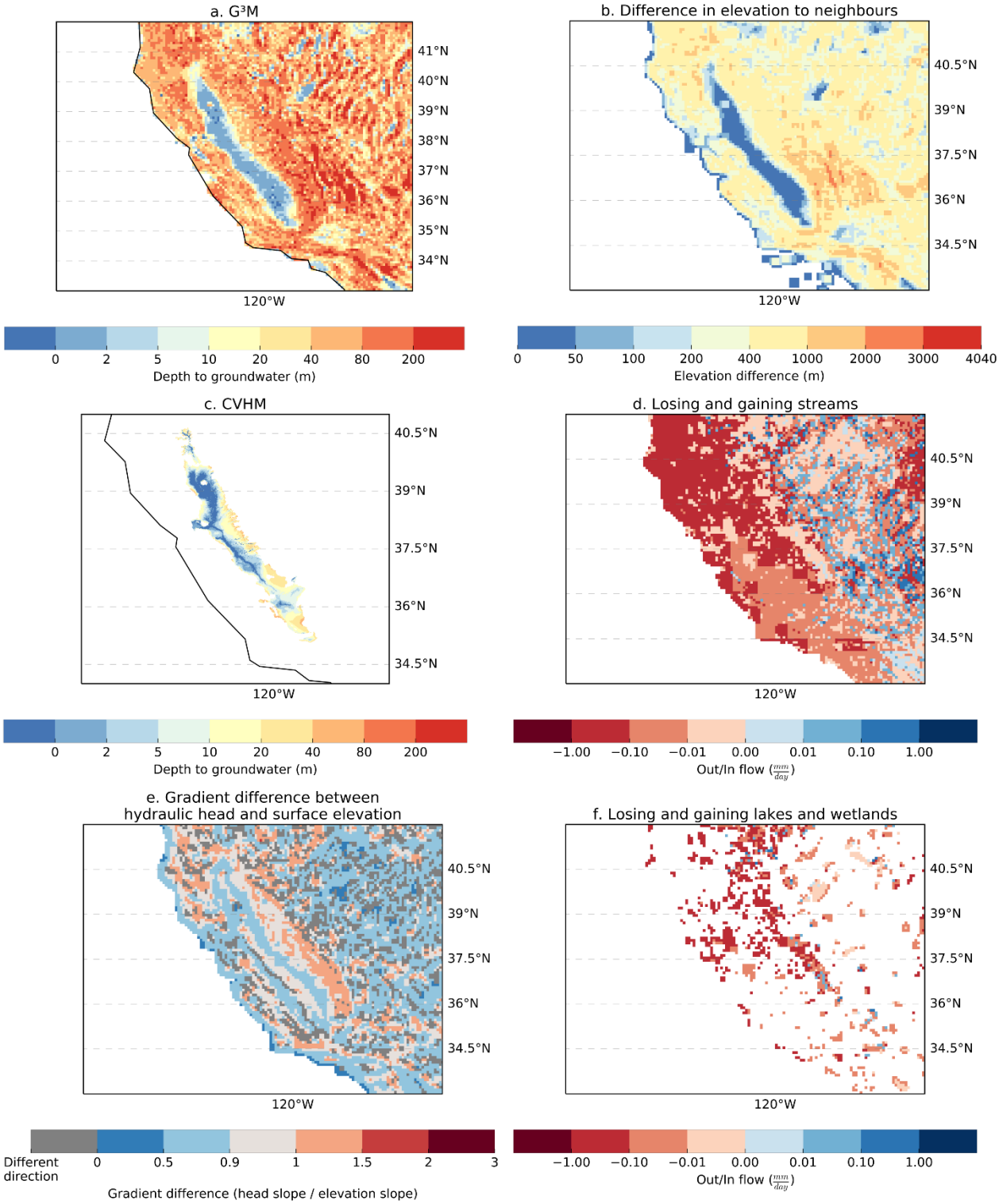

Figure S4.5 Plots of WTD as calculated by G³M (a), difference in surface elevation to neighbouring cells (b), WTD as used by the CVHM as the natural state and starting condition (Faunt, 2009) (c), losing and gaining streams as calculated by G³M (d), difference in gradient of hydraulic head and surface elevation (e), losing and gaining lakes and wetlands as calculated by G³M for the Central Valley and the Great Basin.

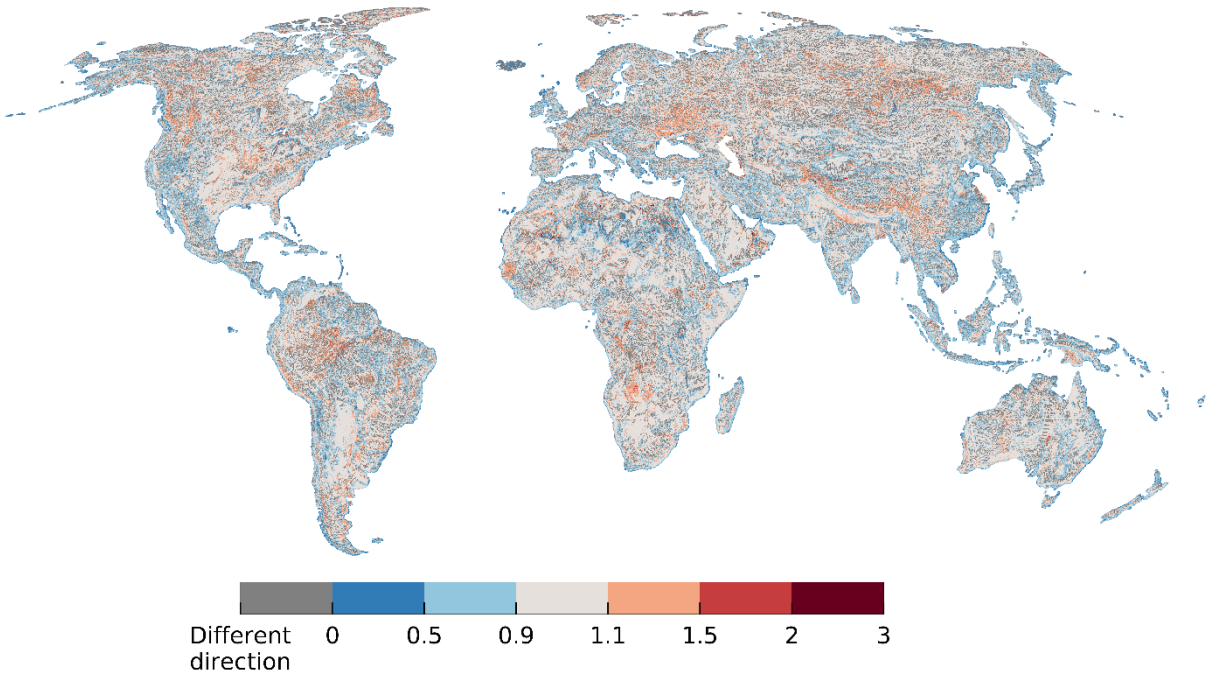

Figure S4.6 Ratio of hydraulic head gradient to 5' mean surface elevation gradient, only computed if the difference in direction of the gradient was smaller than 45°.

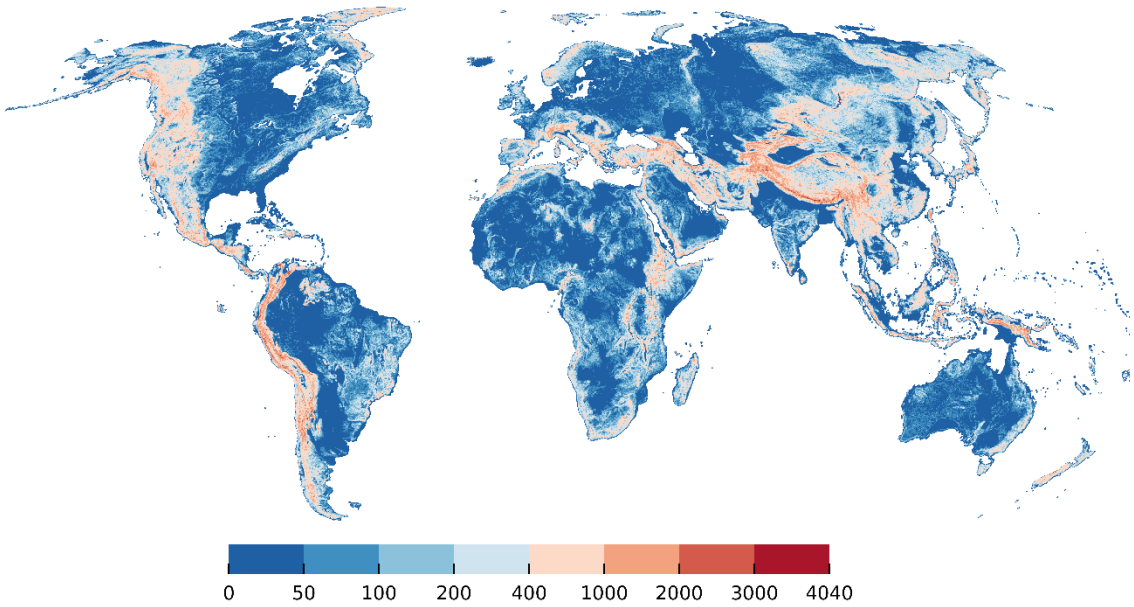

Figure S4.7 Land surface elevation difference between 30" mean land surface elevation in 5' grid cell and mean elevation of neighboring 5' cells [**m**].

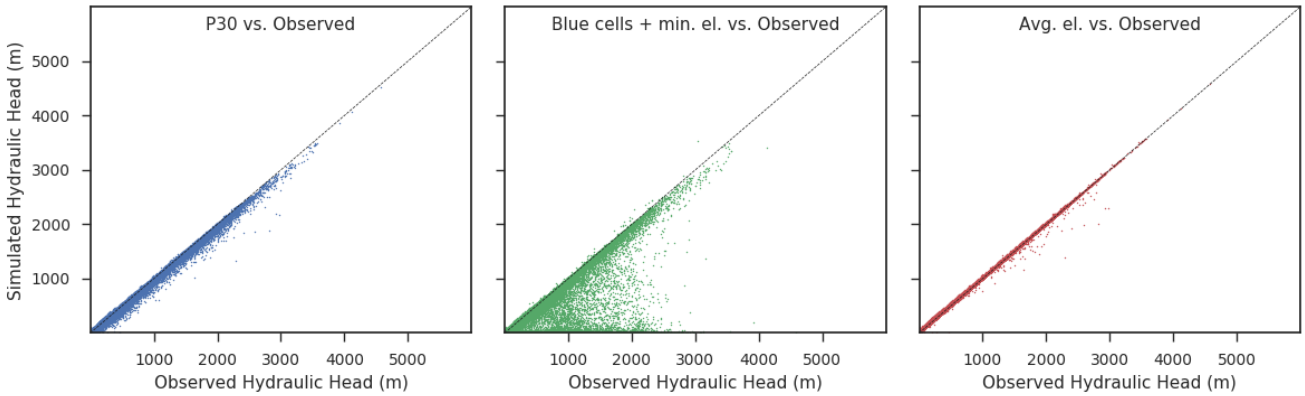

Figure S4.8 Comparison between three alternatives for setting $\boldsymbol{h_{swb}}$. Left to right: Fit of simulated hydraulic heads observations if $\boldsymbol{h_{swb}}$ is set (1) to the 30th percentile of the 30" land surface elevations (standard model) , (2) alternatively to the average elevation of all "blue" cells of the 30" water table results of Fan et al. (2013) or (3) is set to the average of the 30" land surface elevations. A blue cell has a WTD of less than 0.25 m and indicates GW discharge to the surface. If no "blue" cell exists in the 5' cell, the minimum elevation of the 30" land surface elevation values within the cell was used.

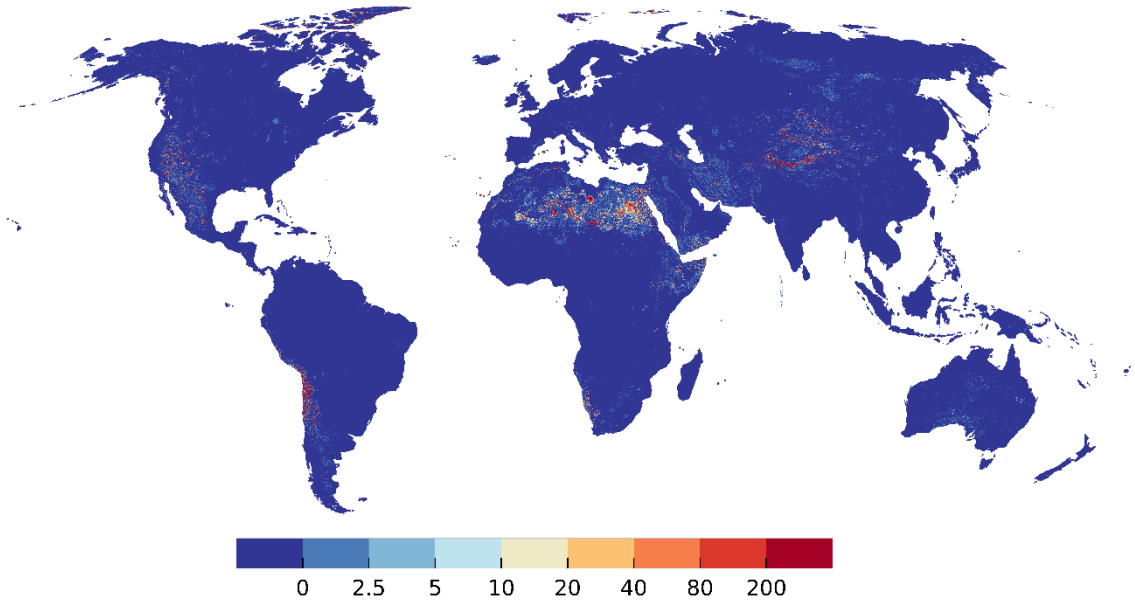

Fig. S4.9 Depth to groundwater [$\boldsymbol{m}$] for SW body elevation $\boldsymbol{h_{swb}}$ at average of 30" land surface elevations.

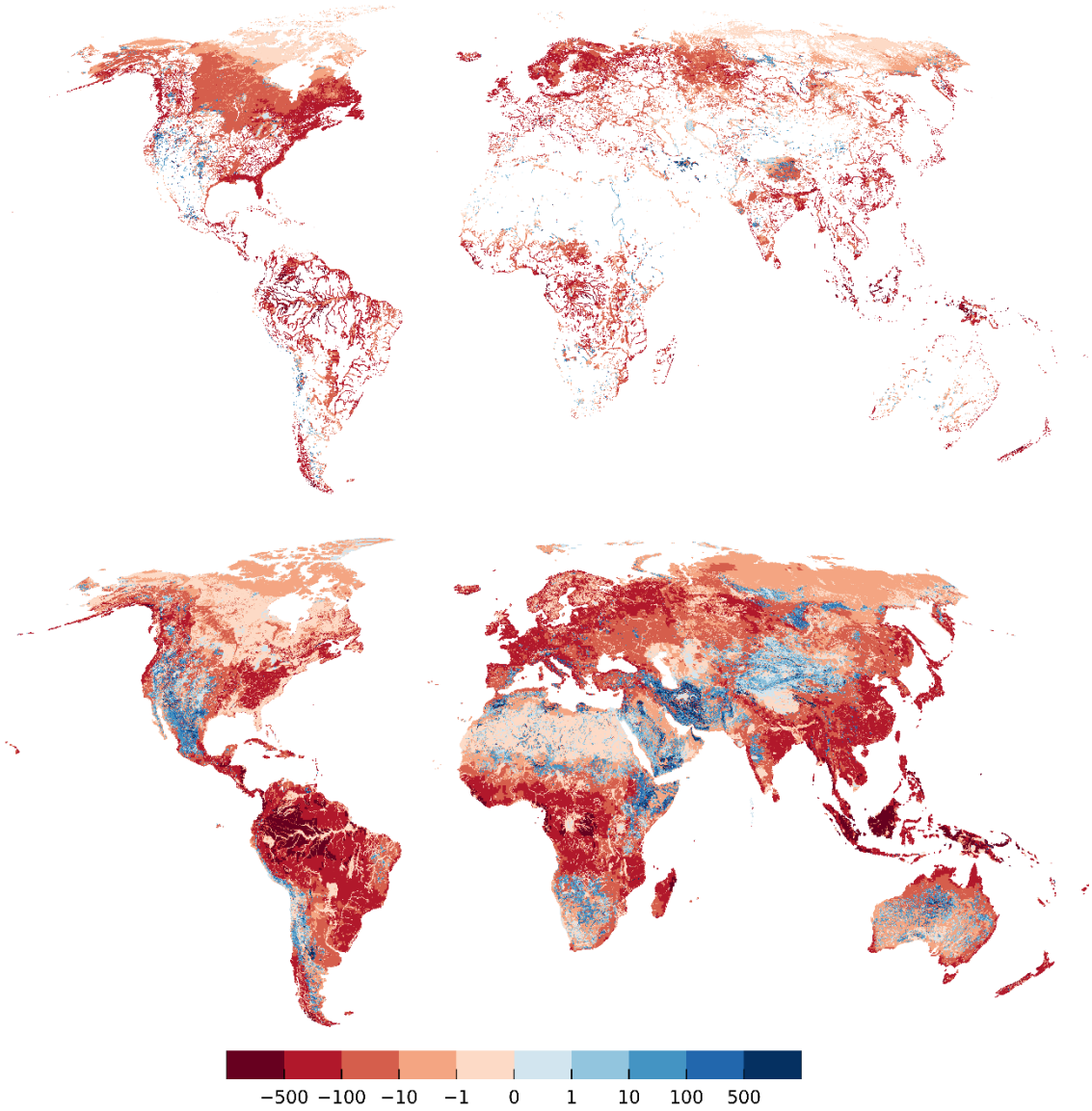

Figure S4.10 Gaining and losing rivers (lower panel) and wetlands and lakes (upper panel) as flow into/out the GW [$\boldsymbol{mm\ year^{-1}}$] if $\boldsymbol{h_{swb}}$ is set to average elevation of all "blue" cells of the 30" water table results of Fan et al. (2013) (right). A blue cell is defined as a depth to groundwater of less than 0.25 m. If no "blue" cell exist in the 5' cell, the minimum elevation of the 30" land surface elevation values is used. Red denotes gaining SW bodies.

References

Alcamo, J., Döll, P., Henrichs, T., Kaspar, F., Lehner, B., Rösch, T., and Siebert, S.: Development and testing of the WaterGAP 2 global model of water use and availability, Hydrological Sciences Journal, 48, 317–337, doi:10.1623/hysj.48.3.317.45290, 2003.

Döll, P. and Fiedler, K.: Global-scale modeling of groundwater recharge, Hydrol. Earth Syst. Sci., 12, 863–885, doi:10.5194/hess-12-863-2008, 2008.

Döll, P., Hoffmann-Dobrev, H., Portmann, F. T., Siebert, S., Eicker, A., Rodell, M., Strassberg, G., and Scanlon, B.R.: Impact of water withdrawals from groundwater and surface water on continental water storage variations, Journal of Geodynamics, 59-60, 143–156, doi:10.1016/j.jog.2011.05.001, 2012.

Döll, P., Kaspar, F., and Lehner, B.: A global hydrological model for deriving water availability indicators: model tuning and validation, Journal of Hydrology, 270, 105–134, doi:10.1016/S0022-1694(02)00283-4, 2003.

Döll, P., Müller Schmied, H., Schuh, C., Portmann, F. T., and Eicker, A.: Global-scale assessment of groundwater depletion and related groundwater abstractions: Combining hydrological modeling with information from well observations and GRACE satellites, Water Resour. Res., 50, 5698–5720, doi:10.1002/2014WR015595, 2014.

Fan, Y., Li, H., and Miguez-Macho, G.: Global patterns of groundwater table depth, Science (New York, N.Y.), 339, 940–943, doi:10.1126/science.1229881, 2013.

Faunt, C. C. (Ed.): Groundwater Availability of the Central Valley Aquifer, California, U.S. Geological Survey Professional Paper, 1776, 225 pp., 2009.

Faunt, C. C., Sneed, M., Traum, J., and Brandt, J. T.: Water availability and land subsidence in the Central Valley, California, USA, Hydrogeol J, 24, 675–684, doi:10.1007/s10040-015-1339-x, 2016.

Gleeson, T., Moosdorf, N., Hartmann, J., and van Beek, L. P. H.: A glimpse beneath earth's surface: GLobal HYdrogeology MaPS (GLHYMPS) of permeability and porosity, Geophys. Res. Lett., 41, 3891–3898, doi:10.1002/2014GL059856, 2014.

Müller Schmied, H., Eisner, S., Franz, D., Wattenbach, M., Portmann, F. T., Flörke, M., and Döll, P.: Sensitivity of simulated global-scale freshwater fluxes and storages to input data, hydrological model structure, human water use and calibration, Hydrol. Earth Syst. Sci., 18, 3511–3538, doi:10.5194/hess-18-3511-2014, 2014.

Poeter, E. P., Hill, M. C., Lu, D., Tiedeman, C., and Mehl, S. W.: UCODE 2014, with new capabilities to define parameters unique to predictions, calculate w eights using simulated values, estimate parameters w ith SVD, evaluate uncertainty with MCMC, and more, Integrated Groundwater Modeling Center IGWMC, of the Colorado School of Mines, 2014.